Final Report:

Analysis of Sub-Grid Boundary-Layer Processes Observed by the P-3 Doppler Wind Lidar in Support of the Western Pacific Tropical Cyclone Structure 2008 Experiment

Ralph Foster
Applied Physics Laboratory
1013 NE 40th St
Seattle, WA, 98105-6698
phone: (206) 685-5201   fax: (206) 543-2480   email: ralph@apl.washington.edu

Co-I G. David Emmitt
Simpson Weather Associates
809 E. Jefferson St
Charlottesville, VA, 22902
Phone: (434)-979-3571 email: gde@swa.com
Award Number: N00014 08-1-0247.

INTRODUCTION

A major field program to study tropical cyclones in the Western Pacific was jointly funded by ONR and NSF (with international participation from Germany, Japan, China, South Korea, Canada, France, U.K. and Taiwan) as part of the THORPEX Pacific-Asian Regional Campaign (T-PARC). The Tropical cyclone portion of the experiment was called the Tropical Cyclone Structure 2008 (TCS-08) Experiment. The goals of TCS-08 were to study the mechanisms of genesis, development and extra-tropical transition of Western Pacific tropical cyclones. This was a large experiment that involved USAF Hurricane Hunter C-130s, the Navy's P-3, the German Falcon aircraft and the Taiwanese DOTSTAR. The P-3 was equipped with the NCAR Eldora Doppler Radar and a Doppler Wind Lidar (P3DWL) system. This was the first extended deployment of a DWL system to study tropical cyclones. A major goal of this research was to investigate how well the P3DWL performed in the severe weather conditions. A second important goal was to assess the atmospheric boundary wind retrievals obtained from the DWL and to use these data for research into PBL dynamics in tropical cyclone conditions.

Airborne DWLs have a history dating back to the late 1970's. Those early systems were used to study clear air turbulence, convective clouds, and boundary layer winds (jets and complex topography flow). Until the TCS-08 field campaign, there had not been a concentrated effort to devote ~100 flight hours to one significant atmospheric phenomena.

OBJECTIVES

 The P-3 Doppler Wind Lidar (P3DWL) uses the latest version of a coherent Doppler transceiver developed at Lockheed Martin Coherent Technologies. The lidar, with the exception of the scanner, is shown on the top in Figure 1. The scanner is shown on the bottom in Figure 1. The scanner is a bi-axial scanner that enables pointing the beam in any direction within a +-30 degree azimuth window and +- 120 degree elevation window. This scanner design was critical to the success of the DWL's participation in TPARC.

The scanner is programmable and can switch between scanning modes during flight. The standard mode used during TCS-08 was a twelve-point step-stare mode (1 sec. duration at each stare and 1 sec. transition to next look) at 20° off nadir followed by a 5-second dwell at nadir. The twelve-point step stare was used to derive vertical wind vector profiles along the P-3 flight path. These provide the bulk of the data from TCS-08. At nominal P-3 cruising speeds (~100 m s^{-1}), the wind profiles are representative of the mean flow over approximately 3 km.

After the field program, the primary objective was to assess the quality of the data. Drop sondes from the P-3 were the validation data set. Once a research quality data set was produced, they were used to study the mean flow in the boundary layer and in numerical model data assimilation experiments.

DATA QUALITY ASSESSMENT

Doppler Wind Profiles:

The DWL is a coherent system (1.6-micron wavelength) that depends on atmospheric aerosols for its return signal; the vertical coverage varies from one situation to another. In general, however, the convection and high winds associated with typhoons provided ample aerosols and thus profiles from flight level (usually 3km) to the surface were common. In fact, both penetration through cloud layers and the number and quality of the wind profiles exceeded expectations and thus suggested that optical systems such as the P3DWL are better suited for cloudy target regions than may have been assumed prior to this deployment. This is a major finding of this research. However, strong rain generally precludes wind measurement. For the lowest range gate near the surface, reflection overlaps with the aerosol scattering and it is difficult to separate the signals in an automated manner. Hence, the lowest level for the DWL wind profiles produced for TCS-08 is 150 m. An example of the overlapping aerosol and surface returns in the layer adjacent to the surface is shown in Figure 2. Special processing is possible in this layer adjacent to the surface (LAS).

The DWL operated at 100 HZ. Thus, each 1-sec sampling contains 100 laser shots. The shot pulses are approximately Gaussian with a length of about 90 m and a diameter of about 10 cm. The lidar has a range regard of 4000 m and the data were processed into 50 m gates with minimal overlap. In the standard processing mode, each DWL stare produces line-of-sight (LOS) winds produced every 50 m that are averaged over the backscattered photons from up to 100 laser shots. The closest returning signals are about 300 m from the lidar. If the aircraft location, motion (pitch, roll, and yaw) and the altitude are known, these LOS winds can be navigated in space and converted into vertical profiles of the full 3-D mean wind vectors. Not all shots return to the receiver, so the SNR must be monitored.

Drop sondes are an inherently different measure of the wind from that of the DWL. Usually Sondes are dropped with relatively large spacing between profiles (~60 km). The sondes follow a drifting trajectory and take approximately 2 to 3 minutes to splash. Depending on the relative directions of the flight path and mean wind, the sondes generally sample a very different part of the mean flow. In a strongly sheared and turbulent boundary layer, such as is found in tropical cyclones, the sonde profiles are best considered to be single realizations of the wind. In principle, but never in practice, multiple sonde profiles should be averaged to estimate the mean wind profile. Furthermore, since the sondes follow a slanted path in conditions of both strong horizontal and vertical shear, the near-surface portion of the sonde profile may not be representative of what the near-surface profile would be below the portion of the profile that sampled higher in the atmosphere.

In contrast, the DWL is closer to a mean wind measurement. However, this mean wind is usually sampled from a different volume of air from that of the near-in-time sondes. The spot on the surface traced by the lidar beam in the step-stare mode is a cycloidal pattern to the side of the aircraft. The drop sonde follows the local wind direction, which is often at a large angle to the aircraft track. Depending on the aircraft flight pattern relative to the mean wind, and/or when the horizontal shear along the path is strong, the different volumes of air sampled by the DWL and sondes respectively may have local forces that are of different magnitudes leading to different force balances and consequently different wind profiles.

P3DWL Deployment and Operation During TCS-08

The P3DWL wind profiles represent first-time data from a first-time instrument and the P3DWL performed well, with a few problems, the tropical cyclone environment. The P3DWL was in operation from August 4 to October 8, 2008. The total amount of data retrieved, including ground and airborne, was 171 hours. This includes all of the research flights, the ferry flights to and from Guam and between bases during TCS-08. The research flights included 18 missions with Tropical Cyclones (Nuri, Sinlaku and Hagupit) as targets at different stages in their development.

Early on, a problem was discovered with the bi-axial scanner. When the P-3 flew at sufficiently high altitude, such as during the ferry flights, the scanner froze in position. The scanner returned to normal operation for the following flights. For the lower-level flights (typical research flight altitude was about 3000 m), this was not a problem. Thus, once this problem was identified, the scanner was oriented to look in the nadir direction during the higher altitude ferry flights. A second problem associated with the communication between the lidar and the aircraft state parameters is discussed below.

About 80% of the downward lidar shots had surface returns (although not necessarily near-surface wind vector retrievals). As an example, P-3 research flight 3 (RF03) sampled tropical depression 13W, which was later developed into Typhoon Nuri, from 16 Aug, 2008 22:14 to 03:20 (17th) UTC. The DWL attempted 448 vertical wind profiles compared to 6 drop sondes (Figure 3a). Of these, about 75% retrieved a wind vector at 200 m, though not necessarily a full profile. About half of the profiles retrieved about half of the possible wind vectors (Figure 3bc).

TCS-08 DWL Profiles:

On board the aircraft, the DWL data are stored in multiple files during acquisition, each file is time-coded with the start time and nominally six profiles are stored in each file. When these profiles were first compared with the near-in-time sonde profiles, a major problem became apparent. A hardware problem on the P-3 aircraft produced a time lag in presenting aircraft state parameters to the DWL. The net errors were subtle and interacted in a nonlinear manner with the DWL processing. Generally speaking, the first profiles in each file were much less affected, sometimes not all, than the later profiles in each file.

Solving this problem required developing a method of estimating the correct aircraft parameters from the available data and developing an improved method of estimating the wind profiles from the twelve-point step-stare data. Previously, the vertical wind vector profiles were extracted using the velocity-azimuth-display (VAD) technique. The new method seeks the optimal horizontal wind vector at each

level using a standard optimization tool (Levenberg-Marquardt). A final science quality wind profile data was only produced on August 23, 2010.

The wind profiles include the horizontal wind vector at every elevation where it could be retrieved using the L-M optimization as well as the vertical velocity. Commonly, the wind profiles are broken because certain layer did not return sufficient LOS data to estimate the wind vector. While the DWL appeared to work well in cloudy conditions, rain was a major cause of no retrievals. The signature of rain was usually consecutive layers of downward vertical velocity.

During and after processing, the individual wind profiles were subjectively assessed for quality. The criteria included the number of wind vectors retrieved, consistency between wind vectors in layers of the profile, an estimate of the goodness-of-fit (GOF) parameter from the L-M solution 9low values are better), and, evidence of rain contamination. The profiles fell into one of four categories. Category *A* profiles had more than half the possible vectors, low GOF and vertical consistency. Category *B* profiles were similar to category *A*, but may have some suspect vectors or possible rain effects. Category *C* profiles may have some good vectors, but more suspect ones due to rain or high GOF parameters. Category *D* profiles were either empty, had very few vectors or had strong evidence of rain contamination.

Direct Comparisons with Drop Sondes

The first DWL data check is to compare the DWL profiles in a given data file with the closest in-time drop sonde. Since the separation between the DWL profiles in a given file and the drop sonde can be on the order of 10 km, real spatial variability can contribute to the differences between the different measurements. In addition, as discussed above, the DWL profiles are representative of the mean flow, while sondes are single realizations. However, we do find reasonable consistency between the data sets and generally very good agreement between the sondes and the highest quality DWL profiles.

Typhoon Hagupit (RF17)

Figure 4 shows part of P-3 research flight 17 (RF17), which flew Typhoon Hagupit on 21 September 2008 23:00 to 0700 (22nd) UTC. Each of the yellow boxes in the figure shows the start of a given file of six to eight DWL wind profiles. Figure 5a-c shows the agreement between a drop sonde and 3 DWL profiles taken during a flight path turn in high winds and cloud-free conditions. Similarly, Figure 6a-c compares a drop sondes with three DWL profiles, also in high wind conditions, taken during a turn in rainy conditions. The signature of rain is seen in the strong downward vertical velocities. In both cases, the DWL profiles agree well with the nearest sondes.

One goal of the research is to use the DWL data to analyze PBL structure in Typhoon conditions. In a strong vortex boundary layer flow, the azimuthal and radial wind components are the result of very different force balances and strong nonlinear interactions (Foster, 2009). Data from the same flight (RF17) were rotated into the radial and azimuthal components (using the JTWC best track) along a leg that was about 200 km from the storm center. Much of this flight went azimuthally around the center at a nearly constant radius. Peak azimuthal winds were 30 to 35 m s^{-1} at this range. Figure 7 shows the location of the DWL profiles superposed on the Eldora backscatter plots for different parts of this flight. Note that the plane doubled back along the clear air and resampled regions where drop sondes had been previously deployed. Figure 8 shows various DWL/sonde comparisons and comparisons between DWL groups of closely spaced DWL profiles taken along nearly constant radius from the

center. Note the relatively large variability in the DWL profiles from 01:56 UTC that were acquired between the relatively strong convection on either side of the P-3. The DWL profiles from 02:35 are compared to the sonde that was dropped in the same region about 15 minutes earlier. The azimuthal winds agree well, but the radial winds are substantially different. Figure 9 shows the storm-relative maximum azimuthal and minimum radial wind speeds from the DWL. There is a general trend of higher azimuthal winds toward the rear of the storm.

Scalar Vector Correlation

A standard method for assessing satellite scatterometer surface wind vector winds compared to buoy winds (Freilich and Dunbar, 1999) is to use the vector correlation defined by Crosby et al. (1993). This parameter varies from 0 to 2. Uncorrelated vector data sets have a zero correlation and perfectly correlated data sets have a correlation of 2. Since perfectly correlated vector data sets can have a constant rotational offset or a constant scalar multiplicative difference, a correlation of 2 does not preclude an overall bias between the data sets. Typical values for long-term matchups between scatterometer and buoy winds, which vary from buoy to buoy, are ~1.7 for buoys away from features that can induce large changes in air-sea interaction such as the Gulf Stream. Figure 10 shows the distribution of vector correlation between DWL and sonde wind profiles for this flight. The median value is slightly greater than 1.

Complex Vector Correlation

One weakness of the Crosby correlation is that it does not provide a sense of overall bias between the different data sets. Kundu (1976) developed a complex vector correlation that can identify directional biases between the data sets. The absolute magnitude varies between 0 (uncorrelated) and 1 (perfectly correlated). The complex phase angle provides a speed-weighted estimate of the directional bias between the data sets. As an example, consider the profiles from RF03 (Figure 3). Wind speeds during this flight were between 10 to 15 m s^{-1}. In Figure 3, the DWL profiles obtained near the drop sondes are color highlighted by the magnitude of the Kundu correlation estimated angular bias between the sondes and the DWL. Some of the wind profiles (as standard U and V components) are shown in Figure11. Also shown are the profiles rotated by the Kundu-estimated rotational bias. The suggestion is that there is about a -10° to -20° directional difference between the sondes and the DWL in this case. Figure 12 shows plots similar to Figure 3 for several other research flights during TCS-08. In all cases there appears to be a small angular difference between the different wind products. In some cases the angular bias is positive and in others it is negative. This is likely due to the sampling issues discussed earlier.

Figure 13 summarizes the results of the Kundu correlation analysis for TCS-08 typhoon flight data set. Overall, the speed-weighted angular bias averages to near zero (with a slight negative skewness) and has a spread of about ±20° when DWL profiles of quality A to C are considered. If we restrict the comparisons to just qualities $A\&B$, the width of the angular bias distribution reduces slightly and becomes more symmetric. If we consider only the A quality profiles, the width of the angular bias distribution is considerably reduced. Similarly, the distribution of the absolute value of the Kundu correlation is close to one when only A quality data are considered. As DWL profiles with lower quality ranking are included, the overall correlation tends to decrease. We conclude that if care is taken to quality control the DWL wind profiles, they are well correlated with the sonde wind profiles.

TEST OF K-PROFILE PBL PARAMETERIZATION SCHEME

Research flight RF15 (19 September 2008 00:00 to 07:30 UTC) sampled Sinlaku as it re-strengthened to typhoon magnitude after crossing Taiwan. C-130 flight AF306 1233W also flew through Sinlaku at the same time. Of particular interest, on this flight the P-3 penetrated through a break in the eyewall convection into the storm core at about 04:00 UTC. Consequently, from this flight we have drop sonde data and DWL profiles from about 200 km into the storm center. Due to the proximity to Japan, only half of the storm could be sampled. Furthermore, to the rear of the storm the flow is off-shore, which likely reduced its symmetry. Even with those caveats, we attempted to fit the nonlinear strong vortex boundary layer model developed by Foster (2009) to these data. Because of its common use in typhoon studies, we employed the K-Profile turbulence parameterization. The K-profile closure is the basis for the MRF and related PBL schemes (e.g. Troen and Mahrt, 1986).

Figure 14 shows the P-3 flight path adjusted to 04:00 UTC using a combination of the Japanese Meteorological Agency and JTWC best track data. (The aircraft-based center fix analysis technique of Willoughby and Chemlow, 1982, provided by NOAA HRD was about 50 km in error at this time.) Both the DWL and P3 sonde wind profiles were rotated into radial and azimuthal coordinates and corrected for the ~9 m s^{-1} translation velocity. The radial pressure gradient was estimated from a combination of the drop sonde splash pressures and the P-3 flight estimate of the surface pressure (corrected for a constant bias of about 6.5 mb). The COARE 3.0 drag coefficient model was used (with a maximum value of 2.5×10^{-3}). The K-Profile model parameters were found to best fit the combined DWL and sonde wind profiles. In general, the azimuthal velocities were well fit, but the inflow, especially in the farther radii of the storm was underestimated. Some of this error is likely due to errors in rotating the wind profiles into radial and azimuthal components; however, some of it is due to problems with the K-profile parameterization. Comparisons of the model to a drop sonde at r = 25 km and to DWL and drop sonde profiles at r = 170 km are shown in Figure 15.

Recent research interest has been focused on validating PBL schemes in typhoon conditions. Direct turbulence measurements have been limited in both number and in distance from the inner core. Zhang et al. (2011) made some estimates from available data using a number of methods (that emphasize local, down-gradient turbulent fluxes) and they find values on the order of 20 to 100 m^2 s^{-1} for conditions similar to this example. They also note that K-Profile schemes generally predict much higher maximum eddy diffusivity values (K_{max}) exceeding 250 m^2 s^{-1}. In this simple example, we required $K_{max} \sim 400$ m^2 s^{-1}, which is consistent with the generally overly high eddy diffusivity in the K-Profile family of models. The implication is a tendency for much stronger entrainment into the PBL and often a much stronger "super-gradient" jet magnitude in the upper PBL. Both of these effects are common found in mesoscale model simulations that use this PBL parameterization. We also note that Foster (1997), Foster (2005), Morrison et al. (2005) and Zhang et al. (2008) argue that unparameterized fluxes from organized large eddies (OLE) may be major contributors to the PBL force balance. The high values of K_{max} in the K-profile paradigm is likely an attempt to compensate for these missing contributions from the OLE. The full fluxes should be a combination of the local, down-gradient fluxes and the non-local (non-gradient) fluxes from OLE. The density and quality of DWL profiles in the TCS-08 data may allow us to test these ideas in more detail.

DATA ASSIMILATION

In collaboration Prof. Xiaoxua Pu of Univ. Utah, the usefulness of the DWL profiles on WRF simulations of Typhoon Nuri was explored using both 3D and 4D VAR techniques. Simulations were run for 48 hours and the impact of the DWL profiles on simulated track and intensity was investigated

(Pu et al., 2010). For both 3D and 4D VAR, assimilating the DWL winds reduced a northward bias in simulated track and reduced the low bias in simulated storm intensity (**Figure 16**). In terms of intensity, 3D and 4D VAR performed about equally. However, the track bias correction using 4D VAR was much better. The impact of the DWL winds was greater than the impact of the sondes alone, which suggests that the high density of even incomplete wind profiles is beneficial to data assimilation in tropical cyclones.

EVIDENCE OF ORGANIZED LARGE EDDIES

During the October 8, 2008 ferry flight from Hawaii to the US west coast, the DWL was oriented in a nadir pointing position. Thus, the LOS winds are essentially the vertical velocity. During the flight, visual observation confirmed that cloud streets were present. Cloud streets form in the updrafts associated with boundary layer organized large eddies (OLE), which are aligned mostly parallel to the mean wind direction. The OLE induce strong near-surface along wind perturbations of up to 20% of the mean wind strength as well as an associated overturning circulation that spans the depth of the boundary layer. The coupling between the negative surface wind perturbations and the updrafts induces the nonlocal (that is, not associated with the local down-mean-gradient) fluxes. The overturning contribution generates near-surface convergence into the updrafts.

Figure 17 shows a series of ~14 km long segments of DWL LOS and SNR data along the transect. Initially, the returns are from the cloud tops, although regular patterns of alternating upward and downward velocities can be seen. Farther along the transect, the PBL gets shallower and the sub-cloud circulations are more apparent. It is evident that the PBL in the clear areas between clouds has downward vertical velocities and that the water surface has upward motion near the cloud updrafts. An improved version of the OLE model described in Foster (2005), which was developed during this research, suggests that the wind perturbations induced by the OLE are consistent with the patterns of sea-surface perturbations (**Figure 18**). However, further research is needed to evaluate this further.

IMPACT/APPLICATIONS

The P3DWL flown on a Navy P3 in TCS-08 demonstrated a significant new source of data for the study of the boundary layer in and around tropical cyclones and for the forecasting of tropical cyclones. The lidar provided far more complete and much more numerous vertical soundings within the cloudy environment of typhoons than was expected. The accuracy of the wind vectors met all expectations. We also conclude that the DWL wind profiles are more representative of the mean wind than are the drop sondes. For most studies, the mean wind profile is of more use than the quasi-Lagrangian, single realization sonde profiles. However, The DWL suffers from rain contamination, usually provides incomplete profiles and cannot easily retrieve winds below ~150 m above the sea surface. Specialized processing could be performed for particular cases of interest. Dropsondes are valuable for the temperature and moisture profiles, their ability to resolve the surface layer and their all-weather capability. Data assimilation experiments demonstrated that the density and quality of even incomplete DWL wind profiles has a beneficial impact on both track and intensity forecasts.

There are extensive funded efforts to establish the accuracy and utility of the data collected on four major typhoons during TPARC. In addition, the data is being used to address issue of representativeness of the widely space samples expected from future space-based DWLs. In the near term, plans are in place to fly two or more DWLs in 2010 during the hurricane research with airborne

DWLs for the next 5 years. All of this airborne DWL activity is being done with the expectation of under flying the ESA4 ADM5 planned for launch within the next year or so.

We also plan to continue to analyze these data to complete the research described above. In particular, a complete analysis of the implied PBL structure and comparison to the model of Foster (2009) and assessment of various PBL parameterization schemes will be completed and an analysis of the Hawaii to California ferry leg. These papers are in development.

REFERENCES

Crosby DS, LC Breaker, WH Gemmill, 1994: A proposed vector correlation in geophysics: theory and application, *J Atmos. Ocean. Tech*., **10**, 355-367.

Foster, RC 1997: Structure and energetics of optimal Ekman layer perturbations, *J Fluid Mech* **333**, 97-123.

Foster, RC 2005: Why rolls are prevalent in the hurricane boundary layer, *J Atmos. Sci*. **62**, 2647-2661.

Foster, RC 2009: Boundary-layer similarity under an axisymmetric, gradient wind vortex, *Bound.-Lay-Meteorol*. **131**, 321-344.

Freilich, MH and RS Dunbar, 1999: The accuracy of NSCAT-1 vector winds: comparison with National Data Buoy Center buoys, J Geophys. Res. 104(C5), 11231-11246.

Kundu P, 1976: Ekman veering observed near the ocean bottom, *J Phys. Ocean*. **6**, 238-242.

Morrison I, S Businger, IF Marks, P Dodge, Businger, J, 2005: Observational evidence for the prevalence of roll vortices in hurricane boundary layers, *J Atmos. Sci*., **62**, 2662-2673.

Pu, Z., L. Zhang and G.D. Emmitt, 2010: Impact of airborne Doppler wind lidar profiles on numerical simulations of a tropical cyclone, *Geophys, Res. Letters*, **37**, L05081.

Troen IB and L Mahrt, 1986: A simple model of the atmospheric boundary layer: sensitivity to surface evaporation. *Bound. Lay Meteorol*. **36**, 129-148.

Willoughby HE and MB Chemlow, Objective determination of hurricane tracks from aircraft observations, *Mon. Wea. Rev*., **110**, 1298-1305.

Zhang, JA, Katsaros, KB, PG Black, S Lehner, JR French, WM Drennan, 2008: Effects of roll vortices on turbulent fluxes in the hurricane boundary layer, *Bound.-Lay Meteorol*. **128**, 1573-1472.

Zhang, JA, FD Marks, MT Montgomery, S. Lorsolo, 2011: An estimation of turbulent characteristics in the low-level region of intense hurricanes Allen (1980) and Hugo (1989). *Mon Wea, Rev*, **139**, 1447-1462.

PUBLICATIONS

Refereed Journals:

Pu, Z., L. Zhang and G.D. Emmitt, 2010: Impact of airborne Doppler wind lidar profiles on numerical simulations of a tropical cyclone, *Geophys, Res. Letters*, **37**, L05081, 5pp

Foster, RC 2009: Boundary-layer similarity under an axisymmetric, gradient wind vortex, *Bound.-Lay-Meteorol*. **131**, 321-344.

Conference Proceedings:

Foster, R., G.D. Emmitt, D. Carre, S. Greco, S. Wood, D. Eleuterio, B. Tang and M. Riemer, 2009: Preliminary Look at Boundary Layer Doppler Wind Lidar Wind Profiles From the Tropical Cyclone Structure, 2008 (TCS-08) Experiment, 16th Conference on Air-Sea Interaction . Proc. of the Annual Amer. Met. Soc. Conference, Phoenix, AZ

Emmitt, G.D. and S. Greco, 2010: Airborne Doppler Wind Lidar: investigating tropical cyclones with curtains of wind profiles, Proc. of the Annual Amer. Met. Soc. Conference, 15th Symposium on Meteorological Observation and Instrumentation, Atlanta, GA

Foster, R.C. and G.D. Emmitt 2010: Doppler Lidar wind profiles in TCS-08, 17th Conference on Air–Sea Interaction, 27-30 Sep, 2010, Annapolis MD.

Emmitt, G.D., Z. Pu, K. Godwin and S. Greco, 2011: Airborne Doppler Wind Lidar data impacts on tropical cyclone track and intensity forecasting: the data processing, interpretation and assimilation, Proc. of the Annual Amer. Met. Soc. Conference, 15th Symposium on Integrated Observing and Assimilation Systems for the Atmosphere, Oceans and Land Surface (IOAS-AOLS), Seattle, WA

Emmitt, G. D., K. Godwin and S. Greco, 2010: Advanced Signal Processing for Airborne DWL Data in Severe Weather, Working Group meeting for wind lidar, Destin, Fl., 2-4 February, 2010.

Emmitt, G.D. and S. Greco, 2010: Airborne Doppler Wind Lidar: investigating tropical cyclones with curtains of wind profiles, 15th Symposium on Meteorological Observation and Instrumentation, Atlanta, GA

Emmitt, G. D., K. Godwin and S. Greco, 2010: Advanced Signal Processing for Airborne DWL Data in Severe Weather, Working Group meeting for wind lidar, Destin, Fl., 2-4 February, 2010

Emmitt, G.D., Z. Pu, K. Godwin and S. Greco, 2011: Airborne Doppler Wind Lidar data impacts on tropical cyclone track and intensity forecasting: the data processing, interpretation and assimilation, 15th Symp. Integr. Obs.and Assimi. Syst. for the Atmosphere, Oceans and Land Surface (IOAS-AOLS), Seattle, WA

Figure1: The P3DWL instrument rack is shown on the top and the biaxial scanner is shown on the bottom along with a fairing form reducing turbulence and drag.
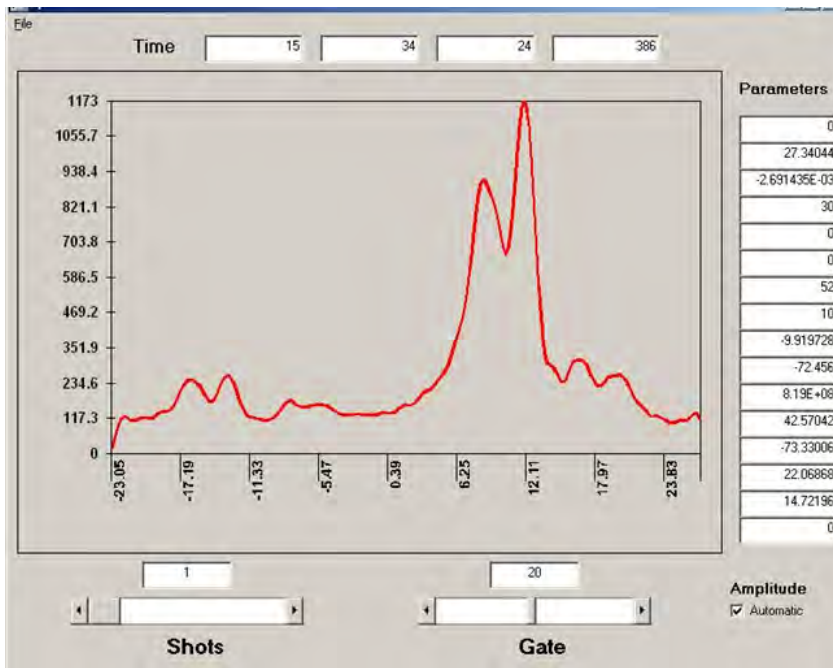
Figure 2: Spectrum for range gate 20 associated with data taken at 33 degrees off nadir. The data has not been fully corrected for the aircraft forward motion
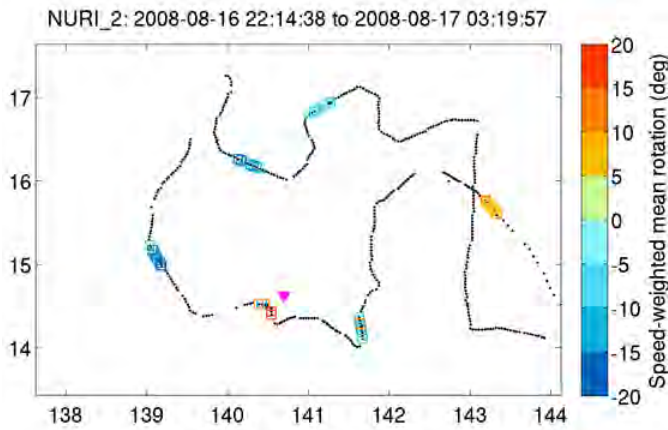
Figure 3: (a) Flight track for RF03. Each dot represents a DWL wind profile. The color highlighted profiles are near the six drop sondes. (b) Cumulative distribution of the number of wind vectors retrieved in each profile from RF03. (c) Cumulative distribution of the lowest DWL wind vector retrieved in RF03.
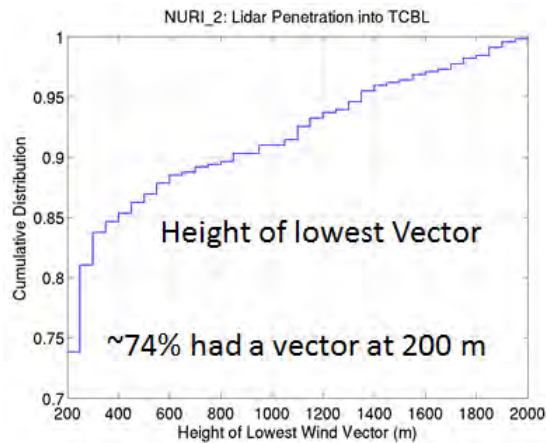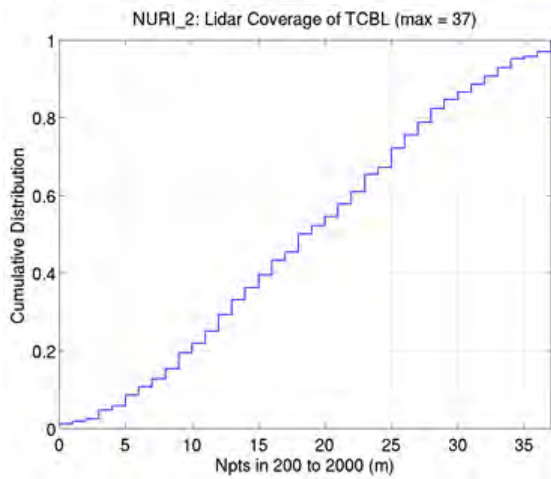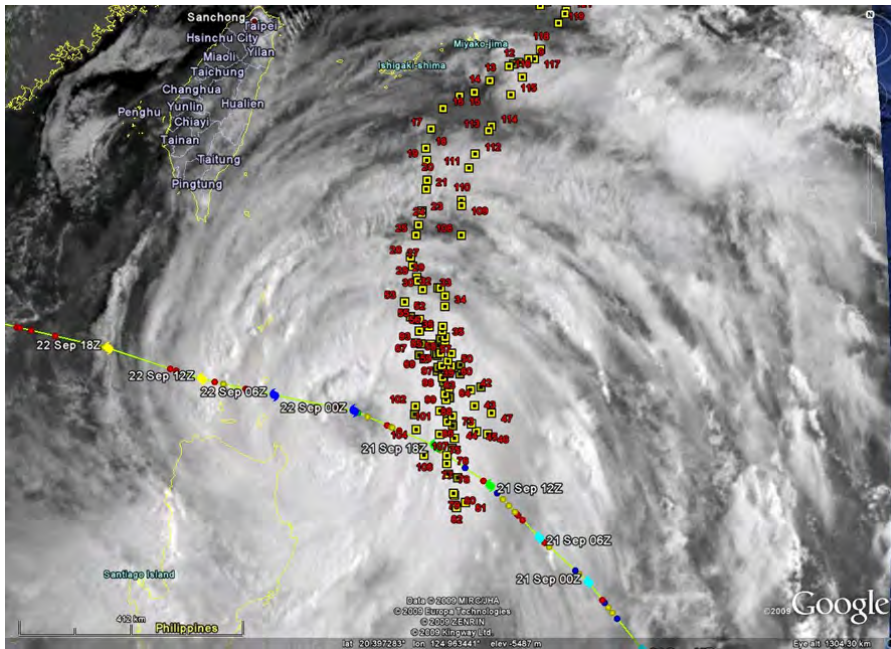
Figure 4: Portion of TCS-08 P-3 RF17 which flew Typhoon Hagupit on 21 September 2008 23:00 to 0700 (22nd) UTC. Each of the yellow boxes in the figure shows the start of a given file of six to eight DWL wind profiles.
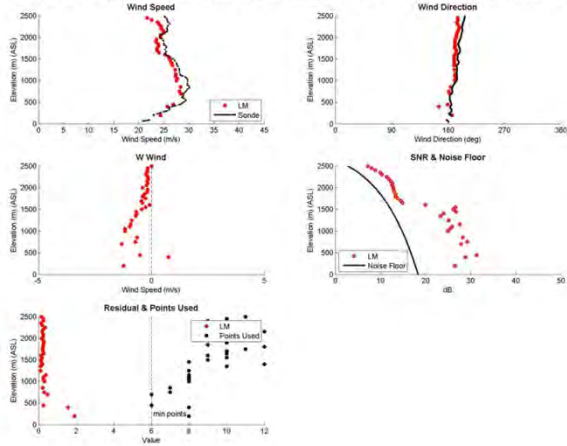
Figure 5: A sequential set of three DWL wind profiles from RF17 taken during an aircraft turn in cloud-free conditions compared to the same drop sonde wind profile.
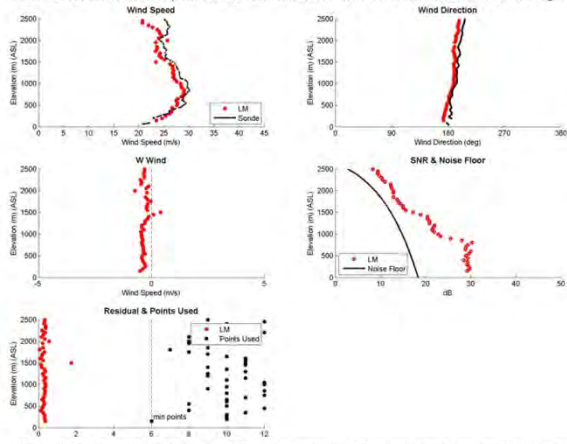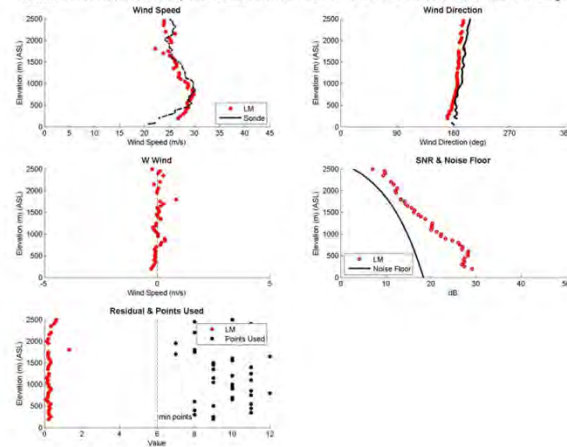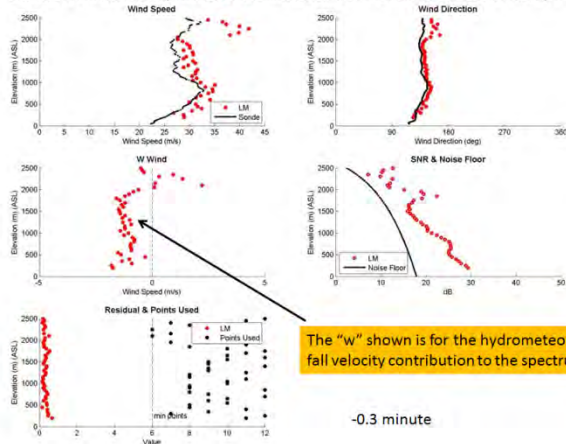
Figure 6: A sequential set of three DWL wind profiles from RF17 taken during an aircraft turn in cloudy and rainy conditions compared to the same drop sonde wind profile.
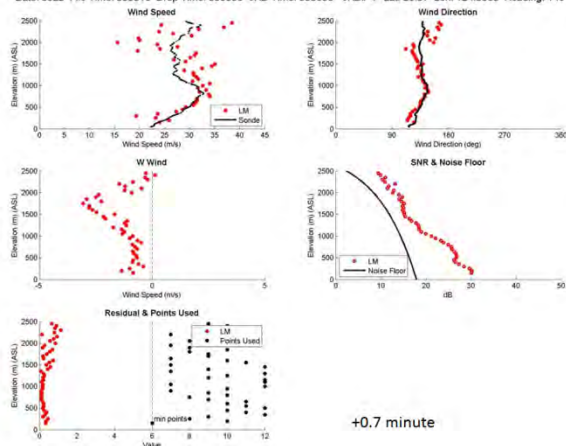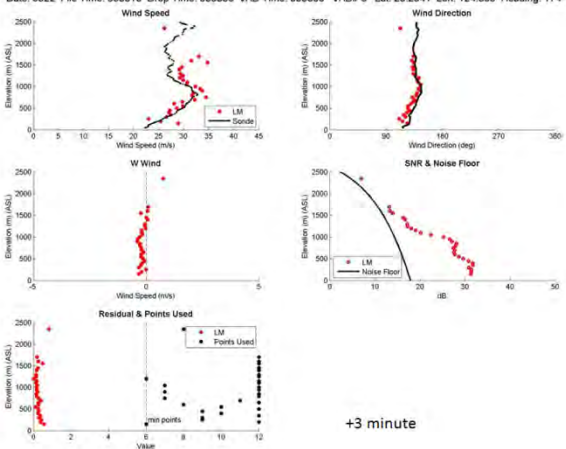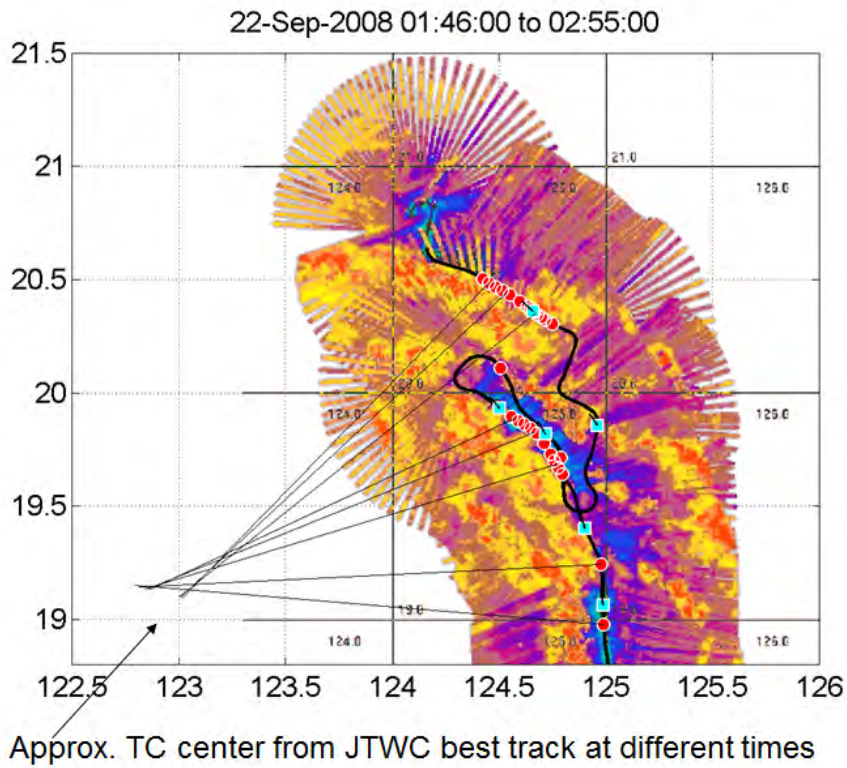
Figure 7: portion of P-3 flight path during RF17 superposed on Eldora backscatter. The DWL profiles are shown as circles and the drop sondes as squares.
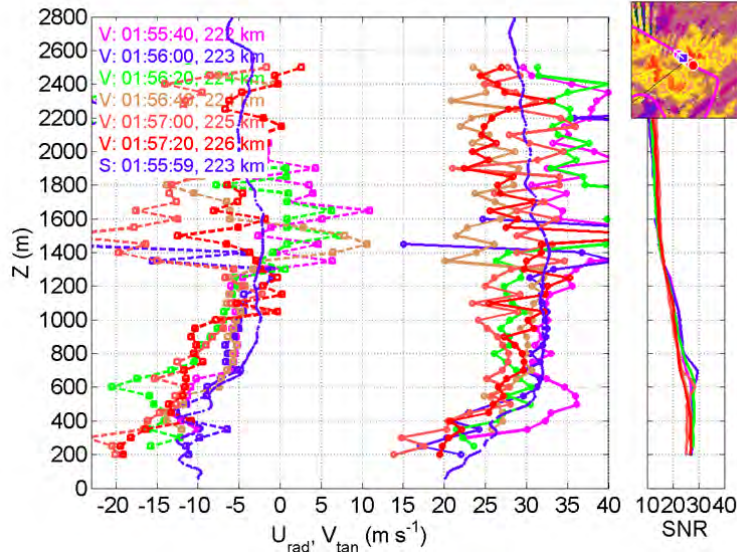
Figure 8: Comparison of Radial and azimuthal wind profiles from the DWL and drop sonde during RF17. (a) Profiles from clear air between strong convection. (b) Comparison of DWL profiles with sonde dropped 15 minutes prior in nearly the same relative location.
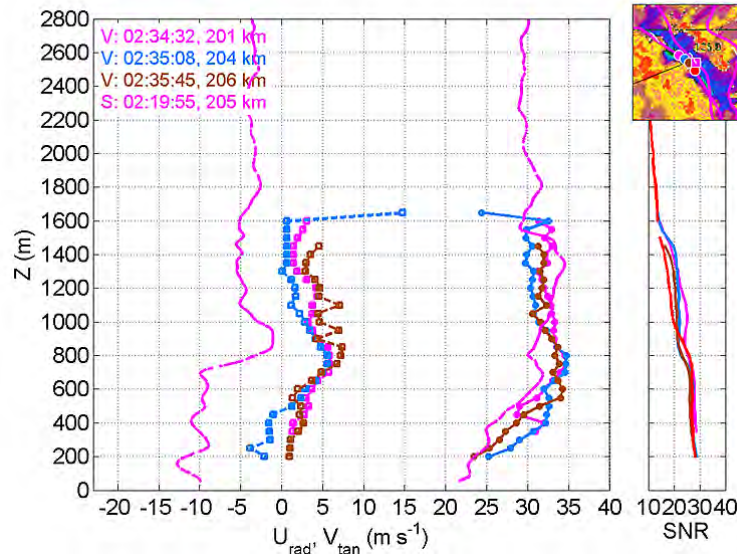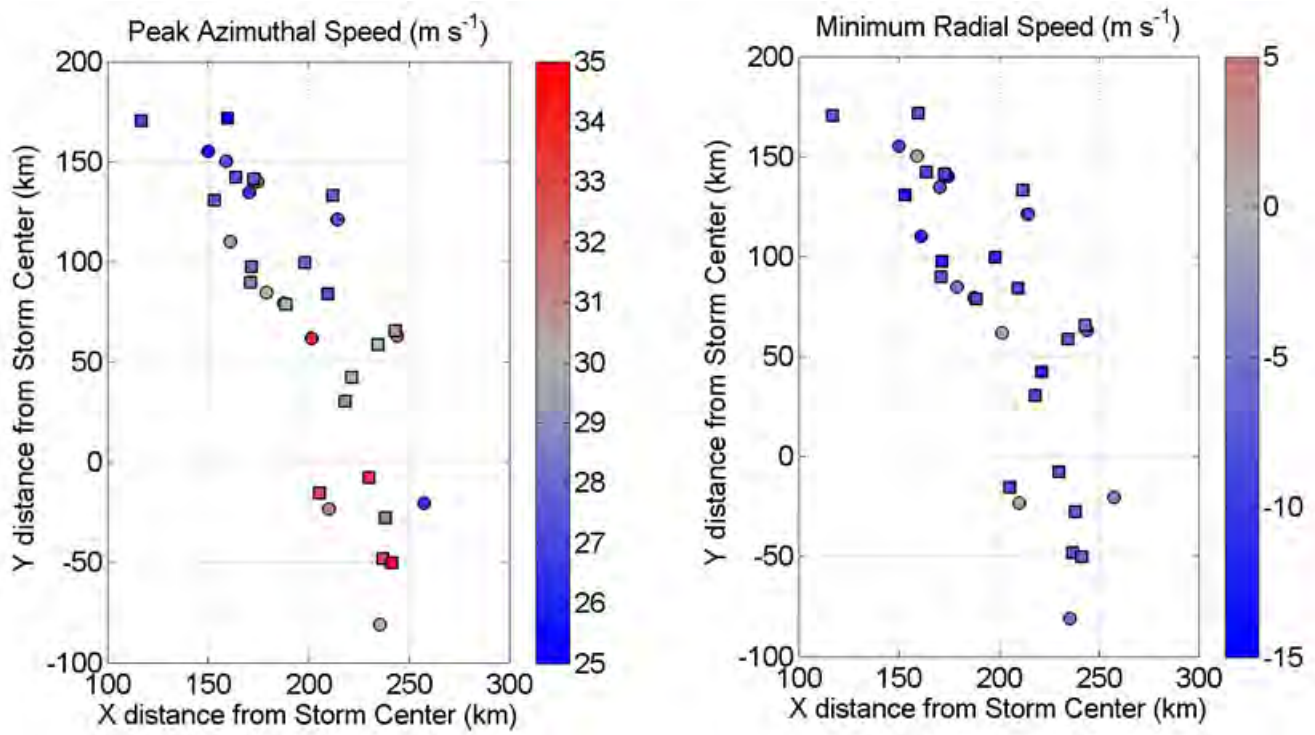
Figure 9: (a) maximum azimuthal wind speed and (b) minimum radial wind speed from DWL profiles during RF17
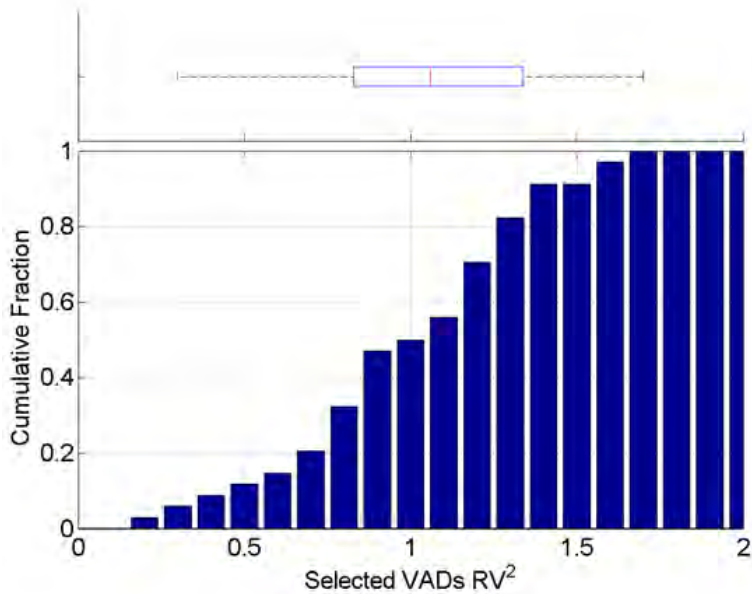
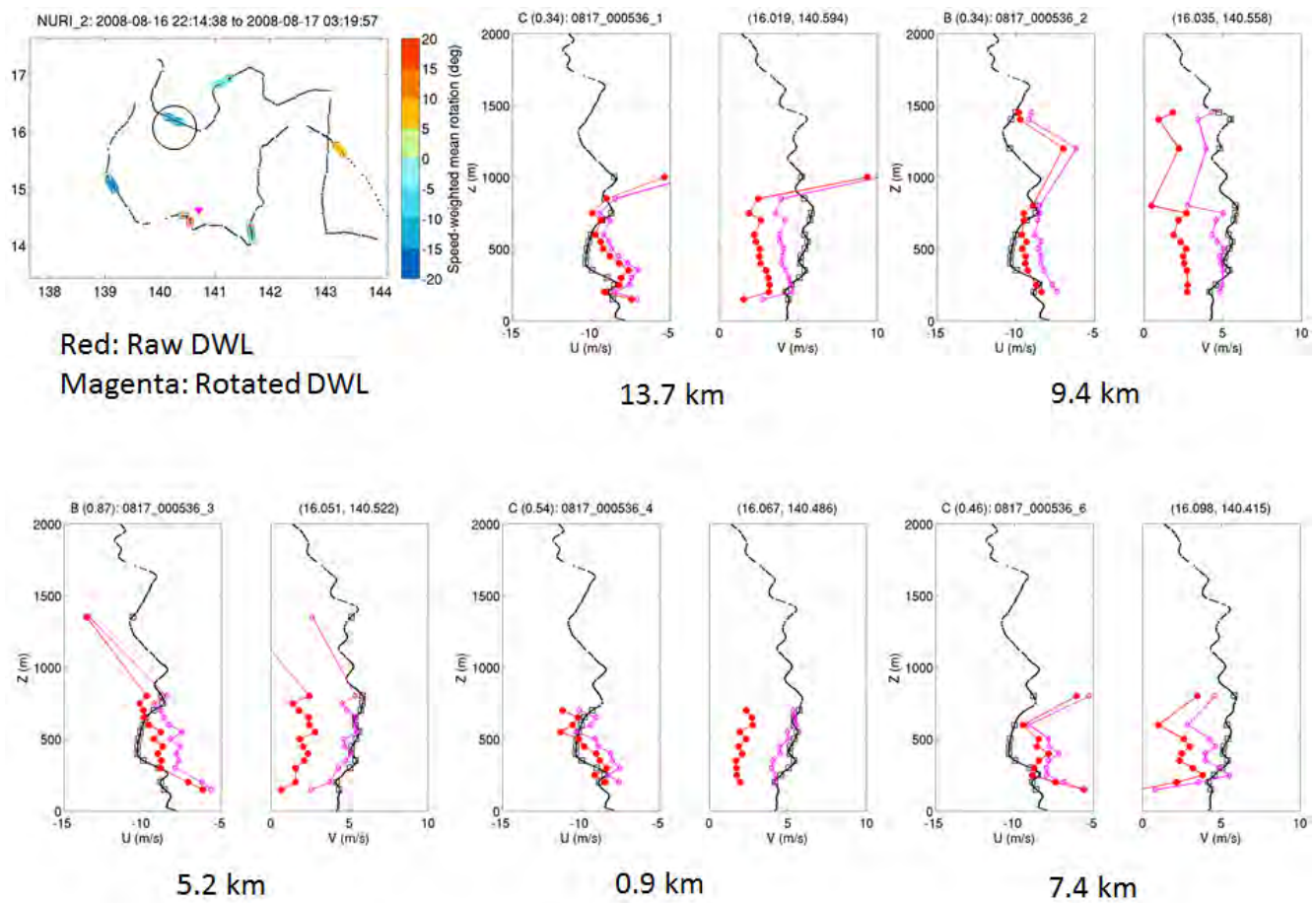Figure 10: Cumulative distribution of the scalar vector correlation between the DWL wind profiles and the drop sondes during RF17.

Figure 11: DWL wind profiles (U and V components separately) compared to the drop sonde circled in the plan view figure. The red curves are the DWL profiles. The magenta curves are the result of rotating the DWL profiles by the speed-weighted directional bias from the complex vector correlation coefficient. The distance below each plot is the distance of the DWL profile from the drop sonde.
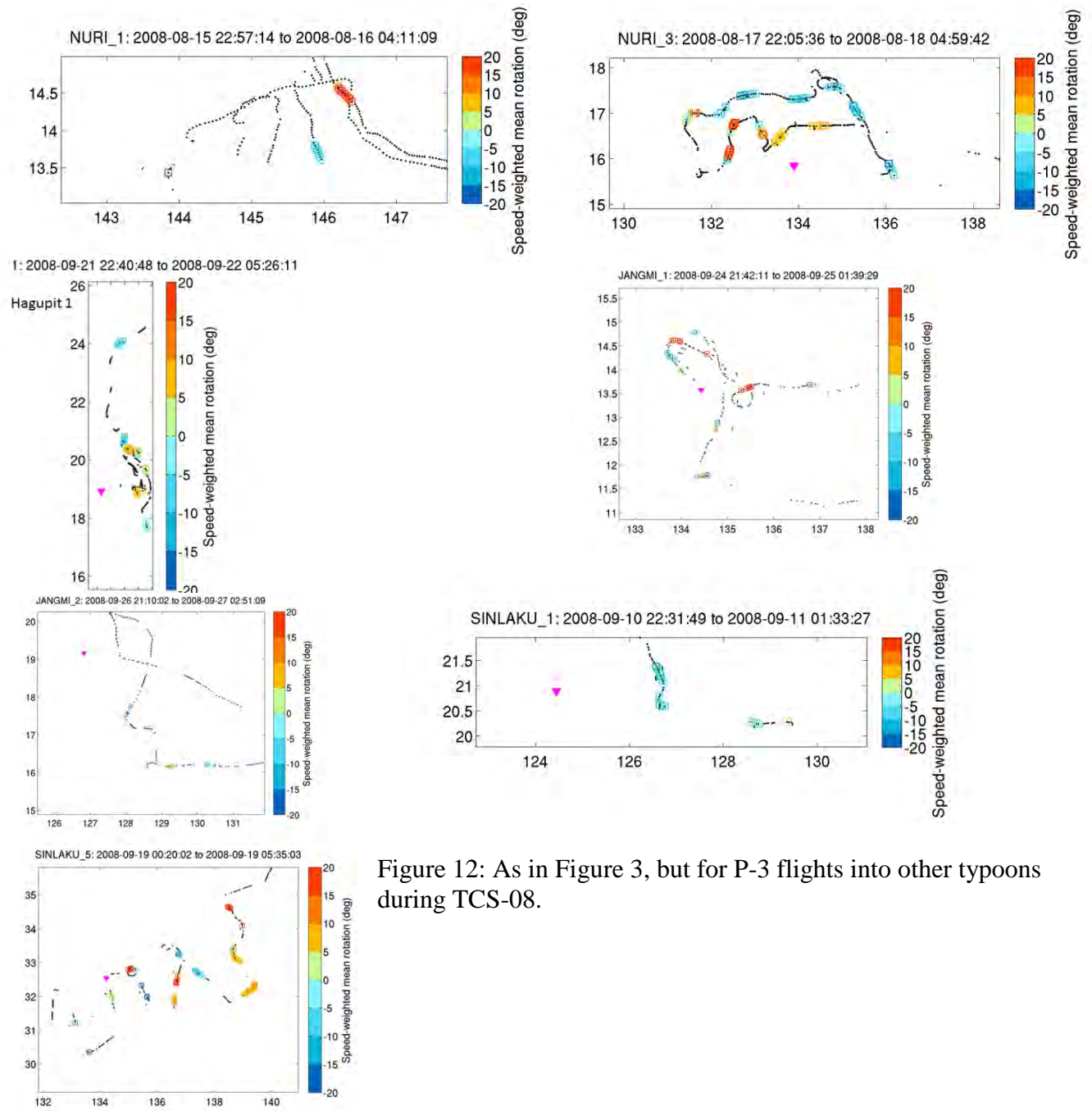
Figure 12: As in Figure 3, but for P-3 flights into other typoons during TCS-08.
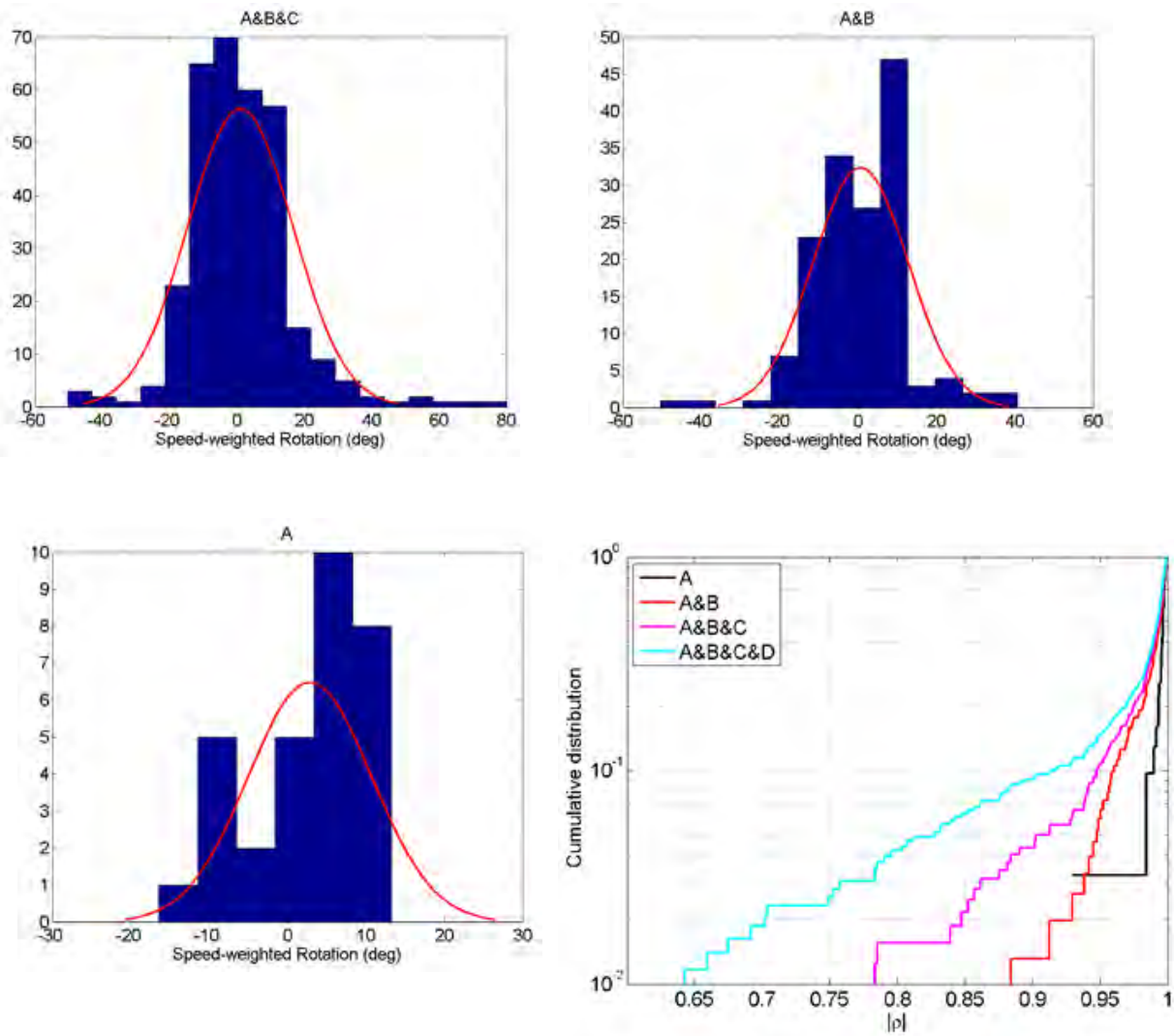
Figure 13: Summary of the complex vector correlation applied to the full TCS-08 data set. (a) Speed-weighted directional bias from DWL profiles of quality ranking A, B and C. (b) As in (a), except for quality A and B only. (c) As in (a) except for quality A only. (d) Cumulative distribution of te absolute magnitude of the complex correlation.
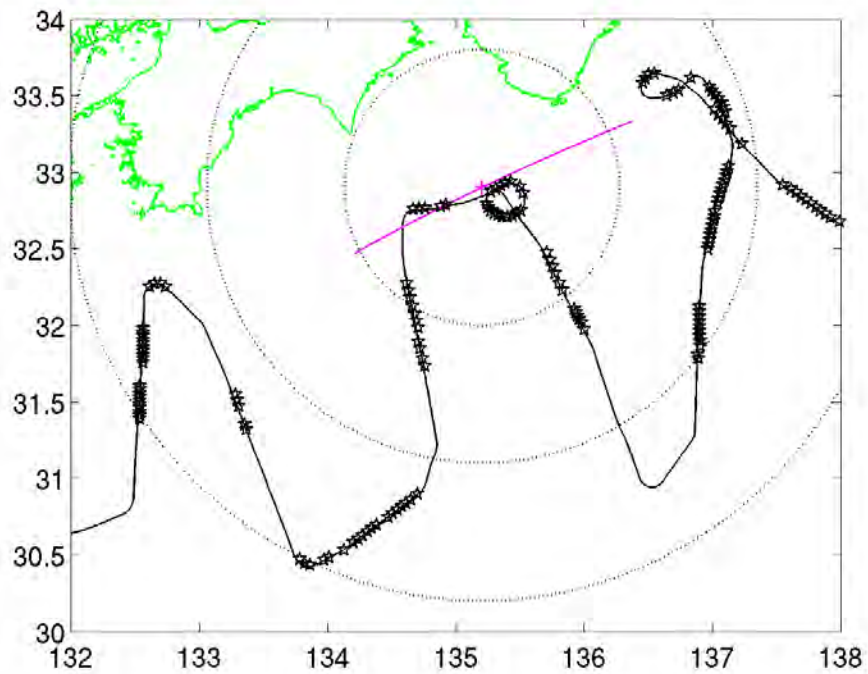
Figure 14: P-3 RF15 adjusted to 04:00 20 Sep, 2008. The stars mark the locations where DWL profiles were attempted.
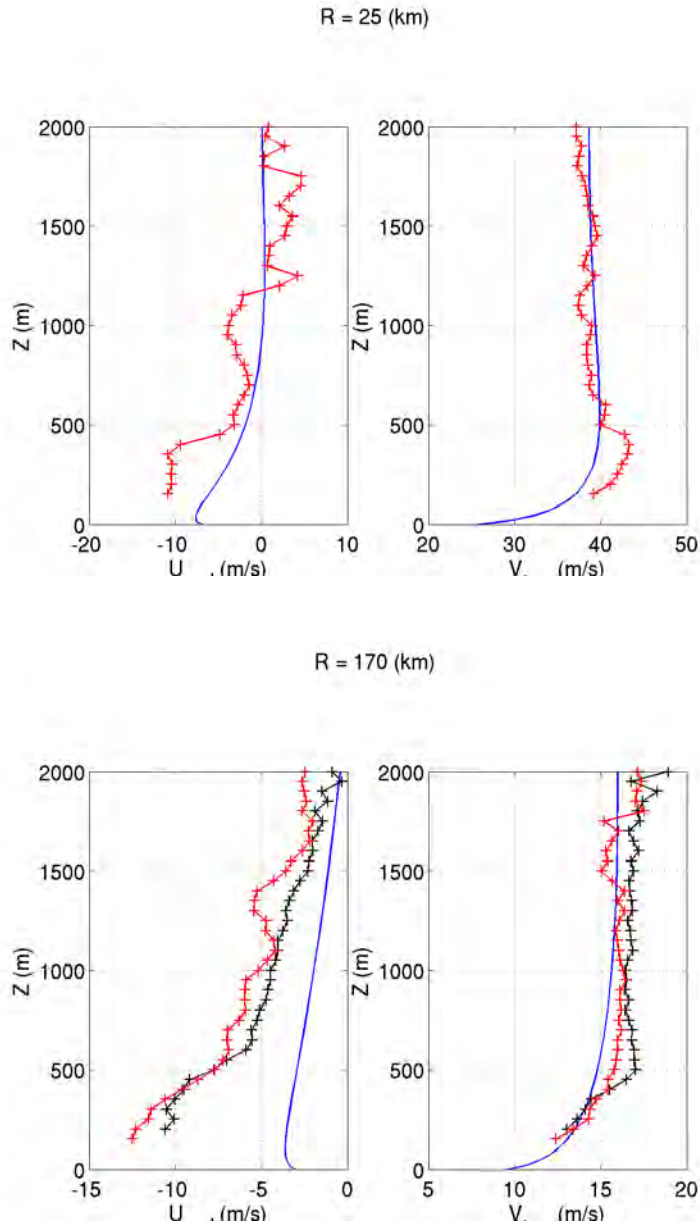
Figure 15: Mean wind profiles (Radial and tangential) from the similarity model (blue) compared to drop sondes (red) and DWL profile (black at (a) r = 25 km and (b) r = 170 km.
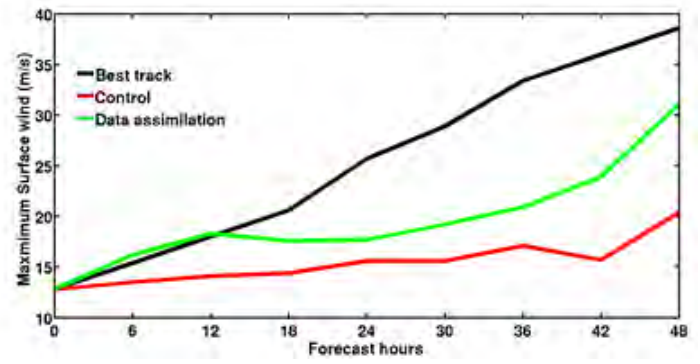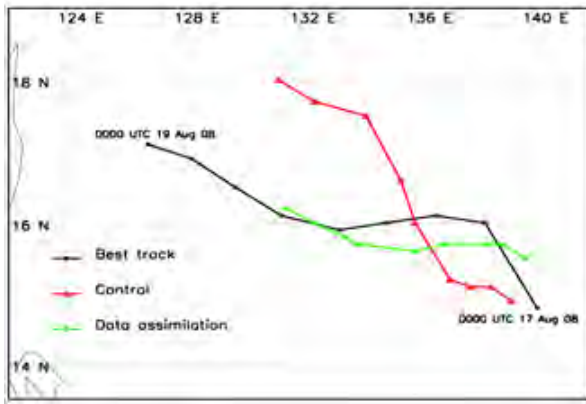
Figure 16: Results from the study of Pu et al. (2010) shoing th eimpact of the DWL wind profiles on (a) track error and (b) intensity error.
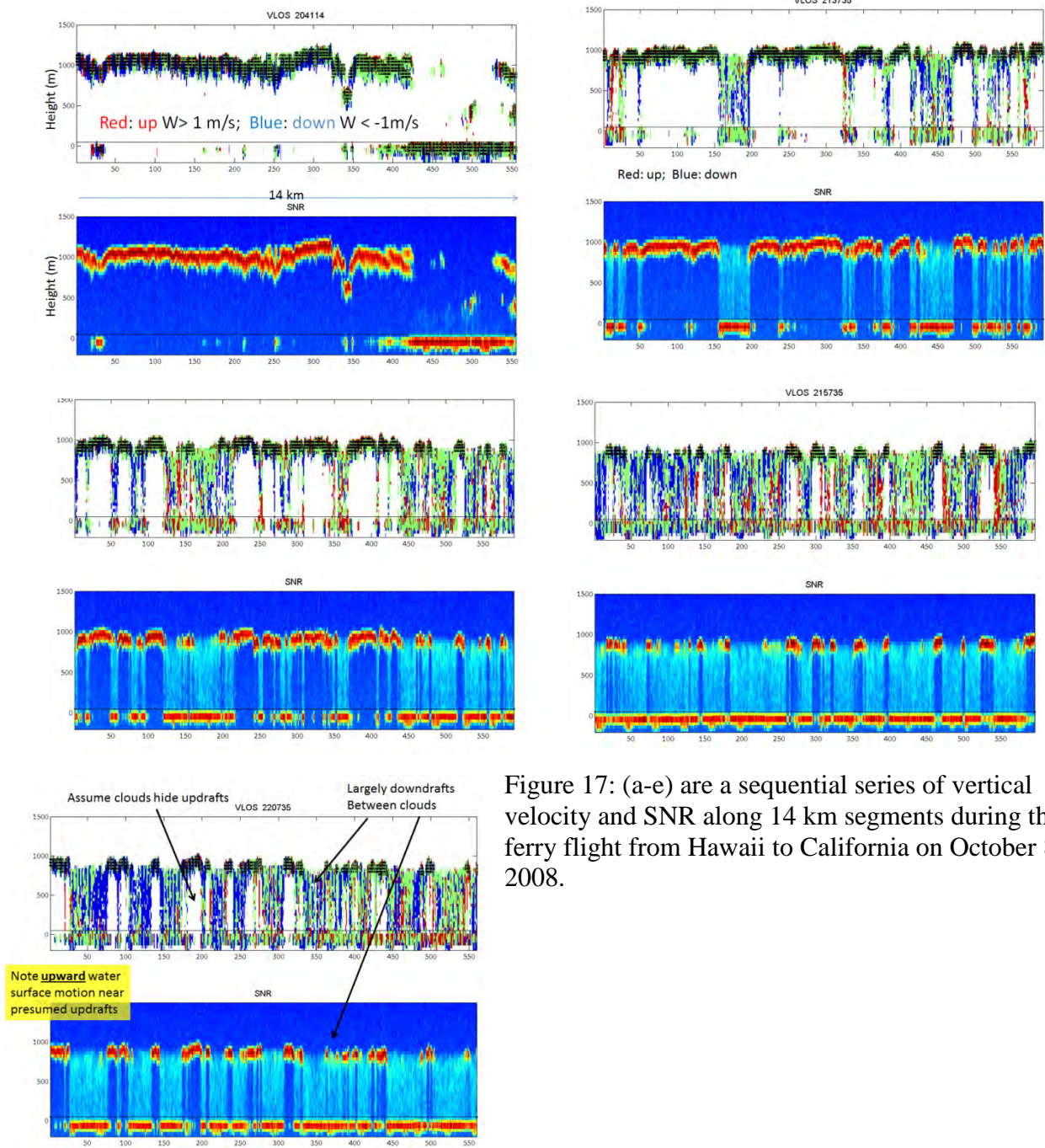
Figure 17: (a-e) are a sequential series of vertical velocity and SNR along 14 km segments during the ferry flight from Hawaii to California on October 8, 2008.
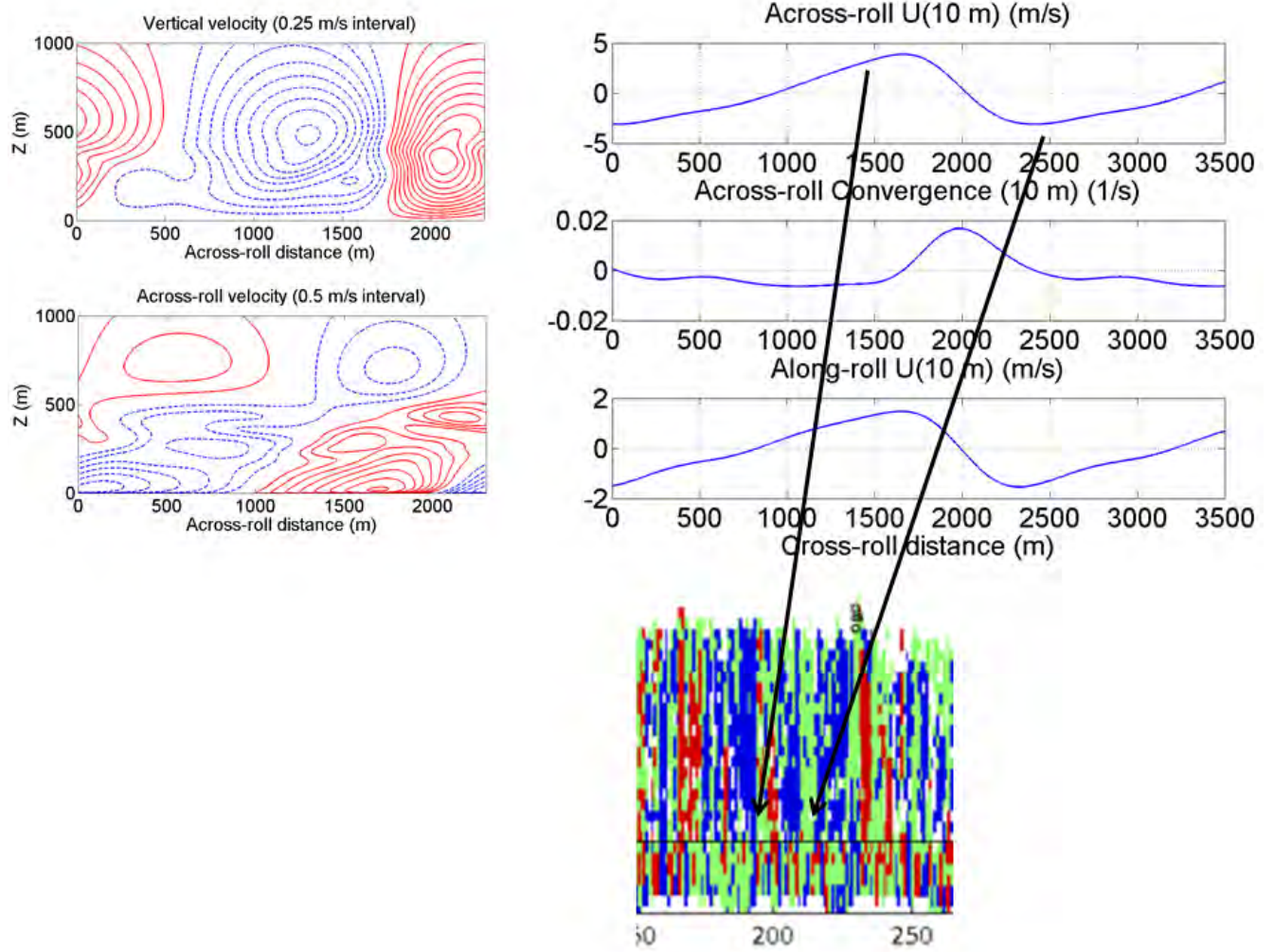
Figure 18: Example output from improved version of nonlinear OLE model developed during this research. Near-surface OLE convergence has similar scale to the near-surface patterns of up and down drafts near the surface seen in the DWL vertical velocity during the October 8, 2008 ferry flight.

REPORT DOCUMENTATION PAGE

The public reporting burden for this collection of information is estimated to average 1 hour per response, including the time for reviewing instructions, searching existing data sources, gathering and maintaining the data needed, and completing and reviewing the collection of information. Send comments regarding this burden estimate or any other aspect of this collection of information, including suggestions for reducing the burden, to Department of Defense, Washington Headquarters Services, Directorate for Information Operations and Reports (0704-0188), 1215 Jefferson Davis Highway, Suite 1204, Arlington, VA 22202-4302. Respondents should be aware that notwithstanding any other provision of law, no person shall be subject to any penalty for failing to comply with a collection of information if it does not display a currently valid OMB control number.
PLEASE DO NOT RETURN YOUR FORM TO THE ABOVE ADDRESS.

1. REPORT DATE *(DD-MM-YYYY)*	2. REPORT TYPE	3. DATES COVERED *(From - To)*
02-02-2012	Final Report	1 January 2008 - 30 September 2011

4. TITLE AND SUBTITLE

Final Report: Analysis of Sub-Grid Boundary-Layer Processes Observed by the P-3 Doppler Wind Lidar in Support of the Western Pacific Tropical Cyclone Structure 2008 Experiment

5a. CONTRACT NUMBER

5b. GRANT NUMBER

N00014-08-1-0247

5c. PROGRAM ELEMENT NUMBER

6. AUTHOR(S)

Foster, Ralph (Univ. Of Washington, Applied Physics Laboratory)
Emmitt, G. David (Simpson Weather Associates)

5d. PROJECT NUMBER

5e. TASK NUMBER

5f. WORK UNIT NUMBER

7. PERFORMING ORGANIZATION NAME(S) AND ADDRESS(ES)

Applied Physics Laboratory - University of Washington
1013 NE 40th Street
Seattle, WA 98105-6698

8. PERFORMING ORGANIZATION REPORT NUMBER

9. SPONSORING/MONITORING AGENCY NAME(S) AND ADDRESS(ES)

Office of Naval Research (ONR 322)
875 North Randolph Street
Arlington, VA 22203-1995

10. SPONSOR/MONITOR'S ACRONYM(S)

ONR

11. SPONSOR/MONITOR'S REPORT NUMBER(S)

12. DISTRIBUTION/AVAILABILITY STATEMENT

Approved for public release: Distribution is unlimited

13. SUPPLEMENTARY NOTES

None

14. ABSTRACT

A major field program to study tropical cyclones in the Western Pacific was conducted as part of the THORPEX Pacific-Asian Regional Campaign (T-PARC). The goals of TCS-08 were to study the mechanisms of genesis, development and extra-tropical transition of Western Pacific tropical cyclones. A major goal of this research was to investigate how well the Doppler Wind Lidar (DWL) installed on the NRL P-3 aircraft performed in the severe weather conditions. A second important goal was to assess the atmospheric boundary wind retrievals obtained from the DWL and to use these data for research into PBL dynamics in tropical cyclone conditions. After the field program, the primary objective was to assess the quality of the data. Drop sondes from a P-3 aircraft were the validation data set. Once a research quality data set was produced, they were used to study the mean flow in the boundary layer and in numerical model data assimilation experiments.

15. SUBJECT TERMS

typhoon boundary layers, Doppler wind lidar, atmospheric boundary layer, organized large eddies, drop sondes

16. SECURITY CLASSIFICATION OF:			17. LIMITATION OF ABSTRACT	18. NUMBER OF PAGES	19a. NAME OF RESPONSIBLE PERSON
a. REPORT	b. ABSTRACT	c. THIS PAGE			Ralph Foster
U	U	U	UU	26	**19b. TELEPHONE NUMBER** *(Include area code)* 206-685-5201

Reset

Standard Form 298 (Rev. 8/98)
Prescribed by ANSI Std. Z39.18